Supporting Information

Electrospray Differential Mobility Hyphenated with Single Particle Inductively Coupled Plasma Mass Spectrometry for Characterization of Nanoparticles and Their Aggregates

Jiaojie Tan,[†,‡] Jingyu Liu[†], Mingdong Li,[‡,§] Hind El Hadri,[†] Vincent A. Hackley,[*,†] and Michael R. Zachariah,[*,‡,§]

[†] Materials Measurement Science Division, NIST, Gaithersburg, Maryland 20899, United States

[‡] University of Maryland, College Park, Maryland 20742, United States

[§] Chemical Sciences Division, NIST, Gaithersburg, Maryland 20899, United States

Table of Contents

Mobility size measurement of AuNPs

For spherical NPs, the mobility size is equivalent to the geometric size. Table S-1 shows a comparison of measured mobility size (by Gaussian fit) with diameter reported by the provider (for reference materials 30 nm AuNP, 60 nm AuNP, and 100 nm PSL, the mobility diameter from DMA analysis as given on the certificate, others are based on transmission electron microscopy). PSL was utilized for calibration of DMA system.

Table S-1

Sample	Diameter by DMA (nm)*	Stated diameter (nm)
Nominal 100 nm PSL (SRM 1963a)	100.1	101.8 ± 1.1
Nominal 30 nm AuNP (RM 8012)	29.7	28.4 ± 1.1
Nominal 40 nm AuNP	42.8	42.4
Nominal 60 nm AuNP (RM 8013)	58.7	56.3 ± 1.5
Nominal 80 nm AuNP	85.2	79.0
Nominal 100nm AuNP	104.4	98.5‾

*The uncertainty of diameter by DMA is consistently less than 1% based on replicate measurements for 30 nm AuNP RM 8012 and PSL SRM 1963a. ‾ The diameter for nominal 100 nm AuNPs is not available from the provider, but the value of a different batch of the same material from the same provider was utilized. The stated sizes for SRM 1963a, RM 8012 and RM 8013 are determined by DMA with an expanded uncertainty representing a 95% confidence interval.

Aggregate Formation

A 4 mL AuNP colloid suspension (40 nm) was centrifuged twice to remove the supernatant containing any excess (unbound) citrate. The centrifuged AuNP suspension was then re-suspended in 1 mL of DI water as a stock suspension, which was confirmed to be colloidally stable over several days. In order to induce aggregation, 50 mmol L^{-1} aqueous ammonium acetate was mixed in equal volume with the AuNP suspension. Prior to conducting single particle measurements by ES-DMA-spICP-MS, the aggregated samples were diluted with 4 mmol L^{-1} AmAc buffer to an appropriate concentration.

Operational Mode of DMA-spICP-MS

Fig. S-2 demonstrates a characteristic "ladder" pattern of increasing intensity for ^{197}Au spikes (i.e., increasing mass or size) with respect to DMA scanning time *t*, (for each DMA voltage step). Overall, for each "ladder-step" within the DMA step time (i.e., 151 s), the DMA operates as a band-pass filter to allow one specific mobility size to exit.

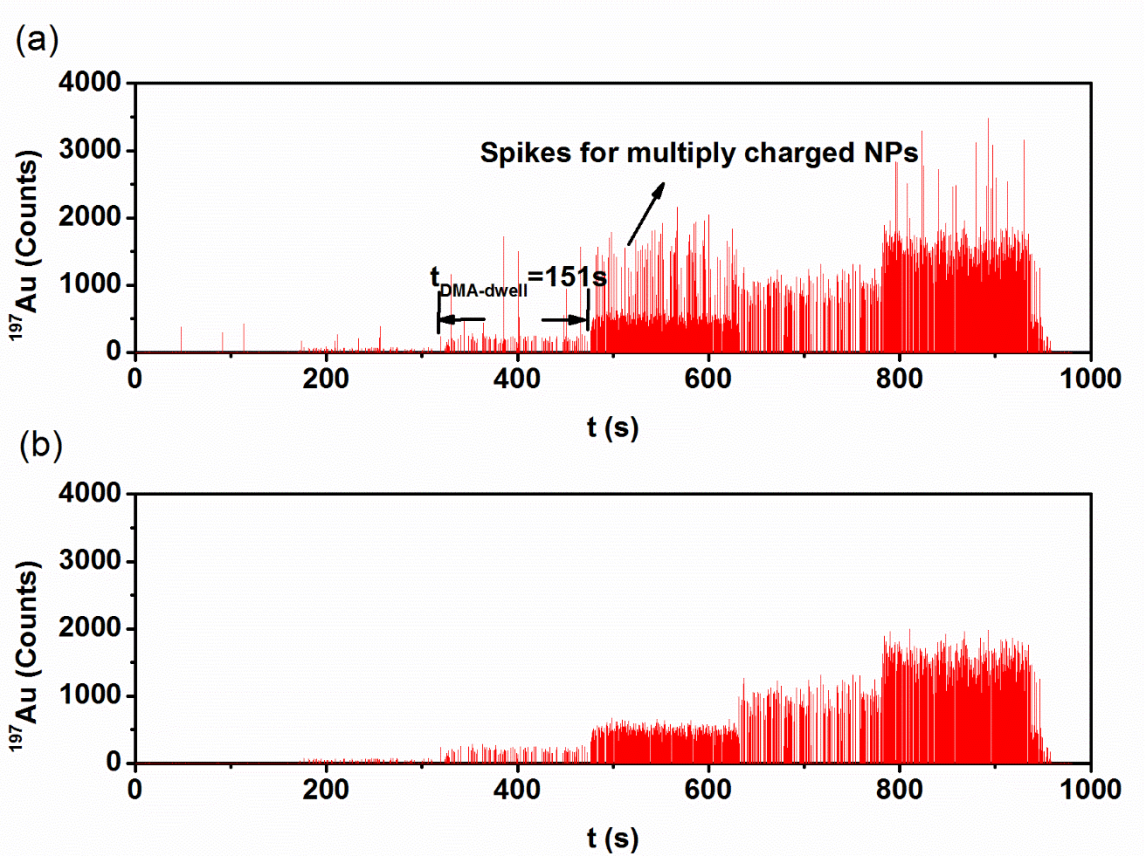

Figure S-2. A mixture of AuNPs containing 30 nm, 40 nm, 60 nm, 80 nm and 100 nm. The DMA selects, with increasing time, 20 nm, 35 nm, 50 nm, 65 nm, 80 nm and 95 nm and with a DMA step time of 151 s at each selected size. (a) Arrow pointing the few higher intensities compared with mostly low intensity spikes from around 480 s to 650 s, representing multiply charged larger NPs. (b) After removing the multiply charged larger NPs with intensity greater than 2σ of the mean intensity for each size step.

Distinguishing NP events

The basic criteria for distinguishing a particle event from the background signal is $I_{particle} > \bar{I} + n\sigma$, where $I_{particle}$ represents the signal from a particle event, $\bar{I}$ is the average intensity (background + particle events), σ is the standard deviation of the average intensity and n is a threshold multiplier set to 5 in this study. A previous study demonstrated that n = 5 is a good compromise between retaining sufficiently high particle counts and minimizing false positives (< 0.1 %). The raw data exported from ICP-MS was recorded as intensity versus time (in counts per dwell time). To process the data, $\bar{I}$ and σ are calculated for the complete data set, and only those pulses satisfying the criteria $I_{particle} > \bar{I} + 5\sigma$ are identified as particle events and subtracted. The same procedure is applied to the remaining data set and repeated until particle events can no longer be distinguished from the background signal. By this method, the particle pulses are separated from the background signal.

Resolving AuNPs from medium containing Au^{3+}

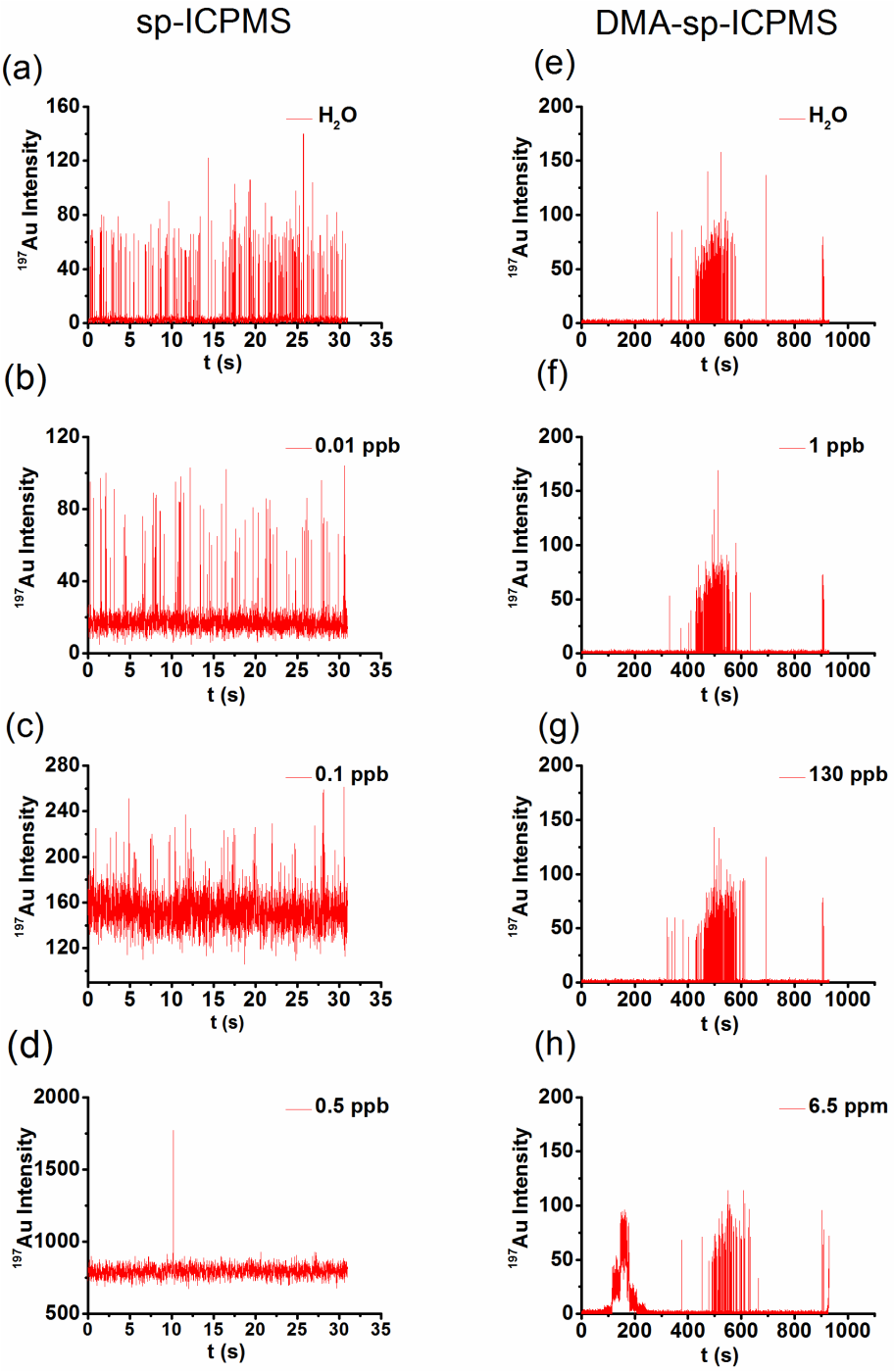

Figure S-3. Time resolved intensity spectrum for 30 nm AuNPs in medium containing Au^{3+} by both stand-alone spICP-MS and DMA-spICP-MS. Dissolved Au^{3+} ranges from 0.01 µg L^{-1} (ppb) to 6.5 mg L^{-1} (ppm) with a fixed AuNP concentration of 0.001 µg L^{-1} (ppb) for stand-alone spICP-MS and 13 µg L^{-1} (ppb) for DMA-spICP-MS. In DMA-spICP-MS, dissolved Au^{3+} is either insignificant (e)-(g) or pre-classified by DMA yielding a small "salt" peak between 0 s and 200 s (h).

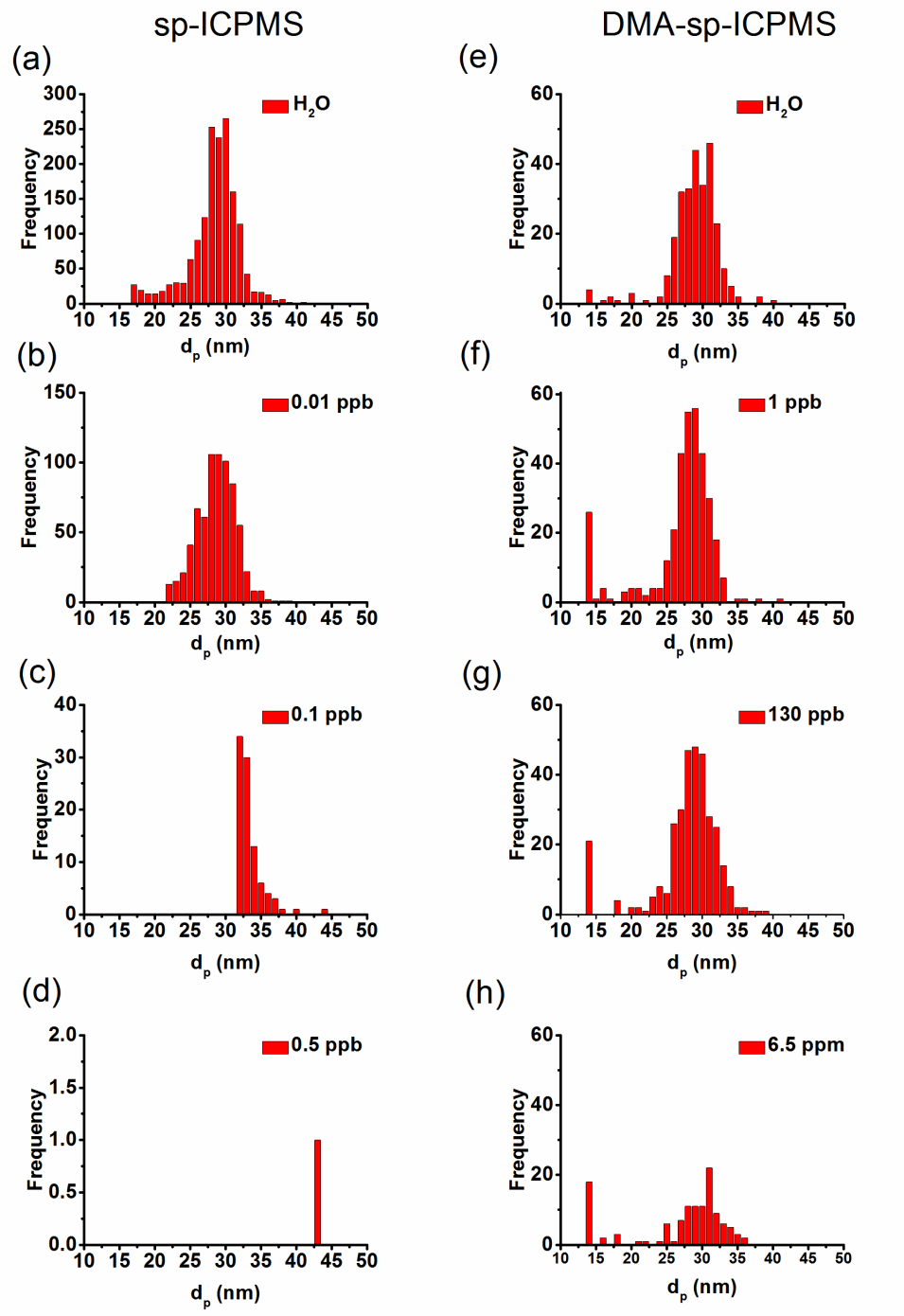

Figure S-4. Particle size distribution for 30 nm AuNP in medium containing Au^{3+} measured by both stand-alone spICP-MS and DMA-spICP-MS corresponding to Fig. S-3.

Transit time from DMA to ICP-MS

In order to obtain the transit time between the exit port on the DMA and ICP-MS detection, the DMA voltage was applied at t=150 s while recording a gradual increase of

^{197}Au intensity until the signal no longer changed. Similarly, the DMA power was turned off at t=330 s to observe the time required for the ^{197}Au signal to decay down to the background value. The response time based on these measurements shown in Fig. S-5 is ≈ 15 s, which we define as the transit time.

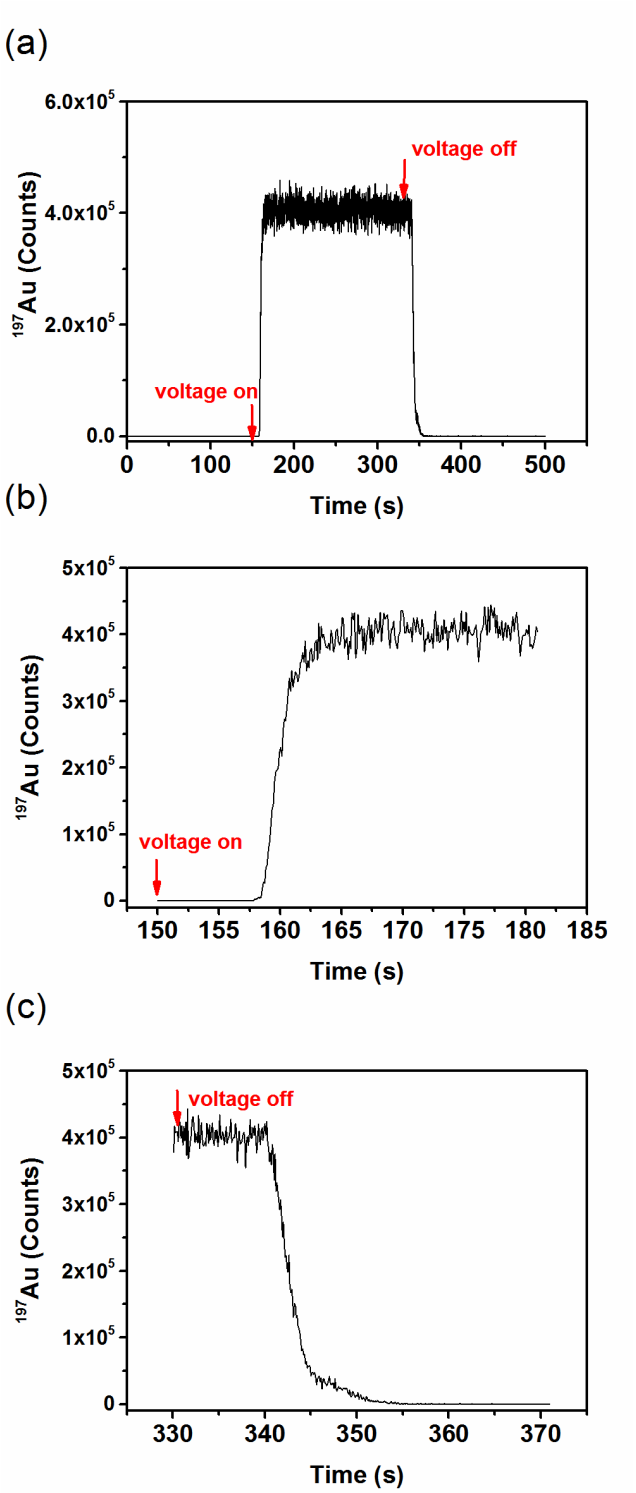

Figure S-5. NP transit time from DMA to ICP-MS obtained by moderating voltage from the power supply; ^{197}Au signal is recorded with respect to time.

Calculation of number concentration

The total number ($N_{spICP\text{-}MS}$) in the aerosol phase detected by spICP-MS was obtained by integrating the peaks for each size NP.

$$N_{spICP-MS} = \int_{d_{m,min}}^{d_{m,max}} \frac{d(N_{raw}/\alpha_c)}{dd_m} dd_m \quad (1)$$

Where d_m represents the mobility diameter selected by DMA, and N_{raw} is the raw number of particles detected by spICP-MS at each mobility size d_m for a fixed amount of time t_{step}, α_c is the probability that a particle is singly charged (which is size dependent and follows Fuchs' charge distribution). $d_{m,max}$ and $d_{m,min}$ are the upper and lower size limit defining the peak. $N_{spICP\text{-}MS}$ is then utilized to obtain the real concentration in solution (*[NP]*) by considering the transfer efficiency for ICP-MS (η_{ICPMS}), DMA (η_{DMA}), and electrospray (η_{ES}), the ES liquid flowrate (f_{ES}), and DMA step time (t_{step})

$$[NP] = \frac{N_{spICP-MS}}{\eta_{ICPMS} \times \eta_{DMA} \times \eta_{ES} \times f_{ES} \times t_{step}} = \left(\frac{N_{spICP-MS}}{k \times f_{ES} \times t_{step}}\right) \quad (2)$$

Where *k* is the total transport efficiency combining the transport efficiencies of ICP-MS (including GED), DMA and ES. Therefore, with a known ES liquid flowrate and DMA step time, from the slope of the concentration calibration curve, which relates NPs detected by DMA-spICP-MS ($N_{spICP\text{-}MS}$) to concentration of NPs in solution, *[NP]*, we can determine the transport efficiency *k*. We calculated k = 12 % under our experimental condition (i.e., 88 % total particle loss). In comparison, as a parallel study using ES-DMA with CPC as the detector, the transport efficiency was determined to be 18 % (i.e., 82% particle loss). Therefore, the majority loss is associated with the front-end of the system (i.e., ES-DMA), which accounted for 94 % of the total particle loss.

Observation of aggregate states at low concentration

Figure S-6 shows the three oligomers representing trimers, tetramers and pentamers. In this case the color scale was reduced so that three distinct peaks are observable (i.e., the aggregates on day 9).

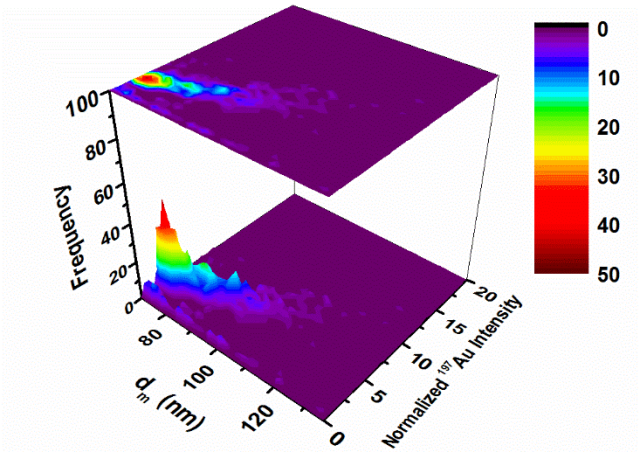

Figure S-6. Observation of aggregate states at low concentration for day 9 aggregation; size axis begins at 70 nm.